Exploration of Otoacoustic Emissions Based on a Single Source Model

Andrew Binder
Dr. Christopher Bergevin, Supervisor

May 8, 2008

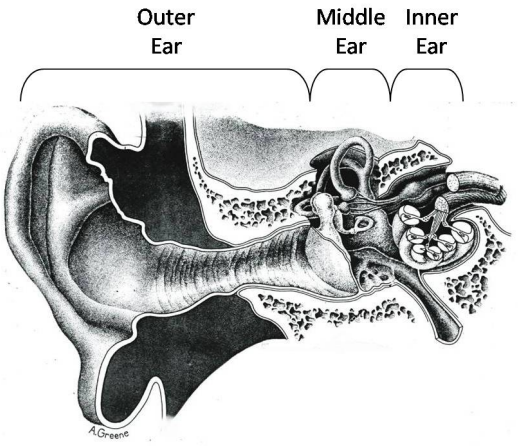

Figure 1: A cross-section of the ear

1 Statement of the Problem

The primary question that forms the basis of this research is whether a single source model is sufficient to explain non-monotonic growth functions found in otoacoustic emission generation. In order to address this question, we explored numerical and analytical approaches to models of distortion product otoacoustic emissions.

2 Overview of Hearing and Otoacoustic Emissions

The primary function of the ear is to convert acoustic stimuli to neural signals. This process can be divided into three sections based on the primary segments of the ear as shown in Fig. 1: the outer ear, middle ear, and inner ear. The outer ear helps to funnel sound to the eardrum and sets it into oscillatory motion. The middle ear transfers the energy from the eardrum to the fluid filled inner ear. The inner ear, or cochlea, then converts this energy into the neural signals. The details of the process that the cochlea uses to achieve this conversion are not well understood. This is caused in part by the tough bone encasing the cochlea. Attempts to cut open the bone to directly observe the process typically damage the sensitive inner ear. Despite this difficulty, there exists a general understanding of the purpose of the individual components of the cochlea.

Inside the inner ear, the basilar membrane partitions the tube-like cochlea along its length into two fluid filled compartments. The energy from the middle ear is transferred to one of these compartments which creates a pressure gradient across the membrane. The basilar membrane has a gradually changing width and thickness. It can be thought of as a series of coupled harmonic oscillators with different resonant frequencies linked by the fluid. The pressure gradient resulting from the energy creates a traveling wave along the membrane that sets it into various degrees of motion. This motion of the basilar membrane in turn affects the organ of Corti. The organ of Corti consists of a fluid with a high electric potential and hair cells. The hair cells have a very low electric potential. When the inner hair cells (IHCs) of the organ of Corti are mechanically stimulated, they open up transducer channels and the hair cell depolarizes. Mechanically stimulating a hair cell requires displacing hair like structures on one end of the cell known as the stereocilia. The depolarization triggers a synapse neuron to fire sending the signal to the brain. The outer hair cells (OHCs), which have a similar structure to the IHCs and far outnumber them, do not appear to have the same function as the IHCs. The OHCs are believed to influence the mechanical stimulation of the IHC bundles.

OHCs are also believed to play a role in a surprising ability of the ear. Experiments show that the ear actually emits sound. These sounds produced by the ear are known as otoacoustic emissions (OAEs). OAEs originate in the inner ear and can be produced in response to a stimulus or spontaneously. The exact source of OAE generation in the cochlea however, is unknown. OAEs are also believed to be related to the amplification function of the cochlea which improves the ear's sensitivity to sound at certain levels. This research seeks to explore characteristics of the generated emissions.

3 Hair Cell Physiology

Outer hair cells (OHCs) are believed to be an important component in otoacoustic emission (OAE) generation. Experiments have shown that when OHCs no longer function normally, OAEs are reduced or no longer produced [1]. The OHC has a very low electric potential, so there exists a potential gradient between the inside of the OHC and its high electric potential environment. Mechanical stimulation, or deflection of the hair cell bundle, opens transduction channels along the stereocilia of the OHC similar to an IHC. Charged particles travel into the OHC to reduce the potential difference. The direction and degree of deflection of the stereocilia determines the number of channels that are opened. Displacement of the hair cell

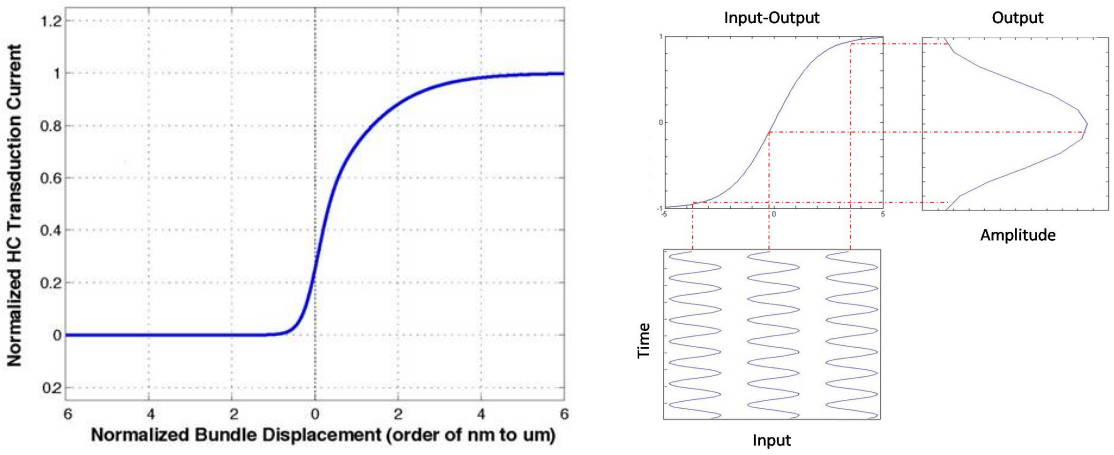

Figure 2: The first graph reveals the sigmoidal, nonlinear relationship between hair cell displacement and the transduction current. The second part of the figure demonstrates the output resulting from sinusoidal waves put through the nonlinearity. It also provides an example of how shifting the operating point of the input-output function affects the output.

bundle in certain directions actually close the transducer channels. The relationship between hair cell displacement and transduction current is nonlinear and is shown in Fig. 2 for a single hair cell. This nonlinearity is believed to be a source of the OAEs and acts as an input-output function for stimulus. The second part of Fig. 2 demonstrates how this transfer function would affect the amplitudes of incoming sinusoidal waves.

The first graph of Fig. 2 that compares hair cell displacement versus transduction current has a sigmoidal shape. The function is asymmetric about its inflection point. A second order Boltzmann function will be used to describe this relationship. The second order Boltzmann function has a sigmoidal shape, is asymmetric, and approaches horizontal asymptotes away from its inflection point. The function has the same characteristics as the graph in Fig. 2. If x is the displacement of the hair cell bundle and y is the normalized transduction current, then the second order Boltzmann function will be

$$y(x) = \frac{A}{1 + e^{b(x-c)} \cdot [1 + e^{d(x-e)}]} \tag{1}$$

where the variables A, b, c, d, and e are dependent upon the physiological characteristics of the hair cells [2]. This equation will be used to describe the input-output function for the sound stimuli.

4 Distortion From a Sigmoidal Nonlinearity

A sigmoidal, nonlinear transfer function implies distortion in the output. A distortion is an alteration of the original input signal. In the case of the hair cell nonlinearity, a distortion of the original frequencies in the input signals is expected due to the nonlinear transfer function. A simple example can be shown to demonstrate that a nonlinear input-output function produces new frequencies. If x represents the two interfering inputs, let

$$x = A_1 \cos(\theta_1) + A_2 \cos(\theta_2) + x_{op} \tag{2}$$

where A is the peak amplitude of the signals. Let $\theta = 2\pi f t$ where f is the frequency of the wave and t is time. Let x_{op} be the operating point of the input-output function. The operating point indicates the center of the range over which the input signals will operate. Fig. 2 shows input signals entered into the input-output function at different operating points. In the ear, the operating point is the resting position of the hair cell bundle. For this example, assume x_{op} is equal to zero. Let the nonlinear transfer function $y(x)$ be

$$y(x) = x^3 \tag{3}$$

Entering Eq. (2) into Eq. (3) and simplifying the result reveals the output to be

$$\begin{aligned} y = {} & \frac{A_1^3}{4}(3\cos(\theta_1) + \cos(3\theta_1)) + \frac{3A_1^2 A_2}{4}(2\cos(\theta_2) + \cos(2\theta_1 - \theta_2) + \cos(2\theta_1 + \theta_2)) \\ & + \frac{3A_1 A_2^2}{4}(2\cos(\theta_1) + \cos(2\theta_2 - \theta_1) + \cos(2\theta_2 + \theta_1)) + \frac{A_2^3}{4}(\cos(\theta_2) + \cos(3\theta_2)) \end{aligned} \tag{4}$$

The results indicate that there are many more frequencies in the distortion output than were present in the input sinusoids. In addition to the input frequencies θ_1 and θ_2, the distortion frequencies $3\theta_1$, $2\theta_1 - \theta_2$, $2\theta_1 + \theta_2$, $2\theta_2 - \theta_1$, $2\theta_2 + \theta_1$, and $3\theta_2$ are present in the output as well.

In order to consider the various distortion frequencies for the Boltzmann input-output function, the Taylor's series will be used to approximate the function in a

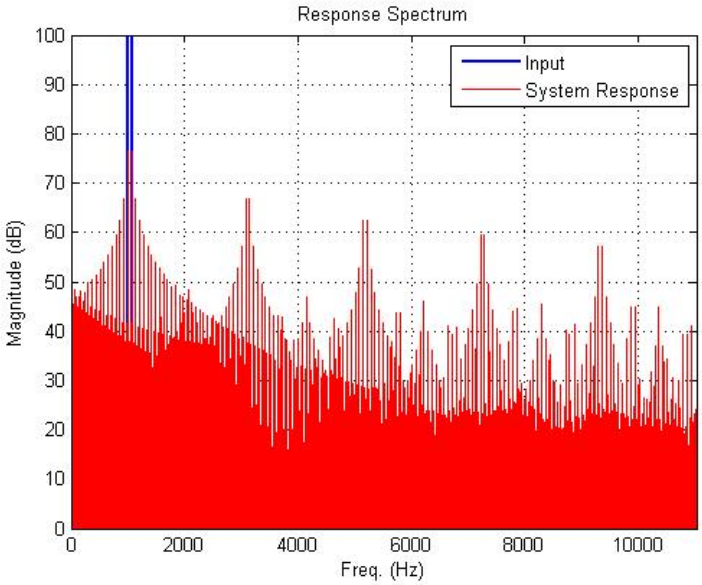

Figure 3: The response spectrum for the output signal resulting from two input signals with different frequencies but the same magnitudes.

polynomial form. If x is equal to Eq. (2), let the second order Boltzmann function $y(x)$ be expanded into

$$y(x) = \sum_{n=0}^{\infty} a_n (x - x_{op})^n \tag{5}$$

where

$$a_n = \frac{1}{n!}[y^{(n)}(x_{op})] \tag{6}$$

We hypothesized that a more complicated nonlinear input-output function such as the second order Boltzmann function should produce a distortion product with an even greater number of frequencies. The basis for this hypothesis is that the output will include the distortion frequencies of x^3 plus the distortions from all other positive powers of x.

A program in MATLAB was used to calculate the distortion frequencies. The distortion frequencies for this sigmoidal nonlinearity are shown in Fig. 3. As predicted, there are many different frequencies in the output signal. Closer examination

reveals that all of these frequencies are some linear combination of the two input frequencies. These results demonstrate that a distortion product OAE (DPOAE) would contain many more frequencies than were present in the input signals. Experimental data does show that linear combinations of the original frequencies are present in DPOAEs [2].

5 Notion of Non-monotonic Growth From this Single Nonlinear Model

Actual data of DPOAEs exhibit non-monotonic growth for increasing levels of stimulus [2]. Non-monotonic growth signifies that there are two or more x-values in a function that yield the same value of y. Non-monotonicity can be determined graphically by observing if it is possible to draw a horizontal line on the graph that will intersect the function more than once. An example of non-monotonic growth is given in Fig. 4. DPOAEs exhibit non-monotonic growth in the form of a notch like the second graph in Fig. 4. It has been hypothesized that this notch is caused by a phase shift of half a cycle in the output. A half cycle phase shift would change the sign of the function and the direction of the graph.

In order to determine if a phase shift or a notch is possible for this sigmoidal input-output function, a Fourier series will be used to provide a spectral representation of the output. A spectral analysis is useful when trying to consider the various frequency, magnitude, and phase components of a function. The Fourier series approximates a function by using an infinite series of periodic functions. Since cosines are being used to model the input sound waves, let the output signal be expanded in a Fourier cosines series only. If $\theta = 2\pi f t$, let the output signal $y(\theta)$ be expanded into

$$y(\theta) \approx \sum_{n=0}^{\infty} a_n \cos(n\theta + \phi_n) \tag{7}$$

where a_n is the nth Fourier series coefficient and ϕ_n is the phase. In this form, a spectral analysis of the output signal is easy to perform. A spectral analysis calculates the magnitude of each distortion product, identifies the frequencies present, and determines the phase of the function. The energy, or amplitude, of each distortion has magnitude a_n. The frequencies are calculated from the $n\theta$ terms inside the cosine functions. The phase is calculated from the argument of the periodic function. A numerical exploration of DPOAE generation and modeling of non-monotonic growth will be performed using this process.

6 Numerical Exploration of Growth Properties of Nonlinear Distortion

The focus of this research is on the relationship between the level, or peak amplitude, of the input sound signals and the resulting magnitude of a distortion product at a specific frequency. A program in MATLAB was used to perform a spectral analysis for two given input signals put through one of the two input-output functions. The fast Fourier transform was used to calculate the magnitude, frequency, and phase of the output. The fast Fourier transform is a computationally efficient method the computer can use to expand a function into a Fourier series in order to perform the subsequent analysis. This spectral analysis can be used to examine how the magnitude of one of the distortion products is affected by a change in the level or amplitude of the input signals. We assumed the amplitudes of the two input signals are equal to each other ($A_1 = A_2$). The process for finding these magnitudes is the same as the process used for the spectral analysis. By performing a spectral analysis of the output signal for a set of input amplitudes, the magnitude of the desired distortion product can be extracted from the spectral analysis. The chosen distortion product has the frequency $2f_1 - f_2$. This distortion product was selected because it is the easiest to consistently measure in an actual experiment. There is more data for this distortion product available for comparison.

The figure from the program should have similar characteristics to the experimental data if this single source model is sufficient for explaining the non-monotonic growth. According to the experimental data, the relationship between the level of the input signals and the magnitude of the distortion product can be non-monotonic. There should be an obvious notch in the graph in the case of non-monotonicity and it should also saturate. Saturation is necessary because there are a limited number of transducer channels that may be open in the hair cell. Therefore, there must be a limit as to how large the output magnitude may become as the input-output function saturates. The output of this program is shown in Fig. 4.

The numerical model shares similar characteristics to the actual data. The output signals have distinctive notches and saturate. The saturation was evident analytically due to the input-output function used. The growth of the function becomes negligible a certain distance from the inflection point due to the second order Boltzmann function's asymptotic limit. Increasingly larger input amplitudes would eventually experience only negligible increases in their magnitude due to the limit. Another common characteristic of both graphs is that the data points leading up to the notch are linear with a slope of three. Since the units are in decibels, this means that the

growth of the magnitude is cubic before the notch. The graph of the phase cycle also reveals that the phase does change by half a cycle at the notch. At this point in the graph, the function changes signs. A change in sign of the cosine function requires a phase shift of π or half of a cycle, which is shown in the phase cycle graph in Fig. 4.

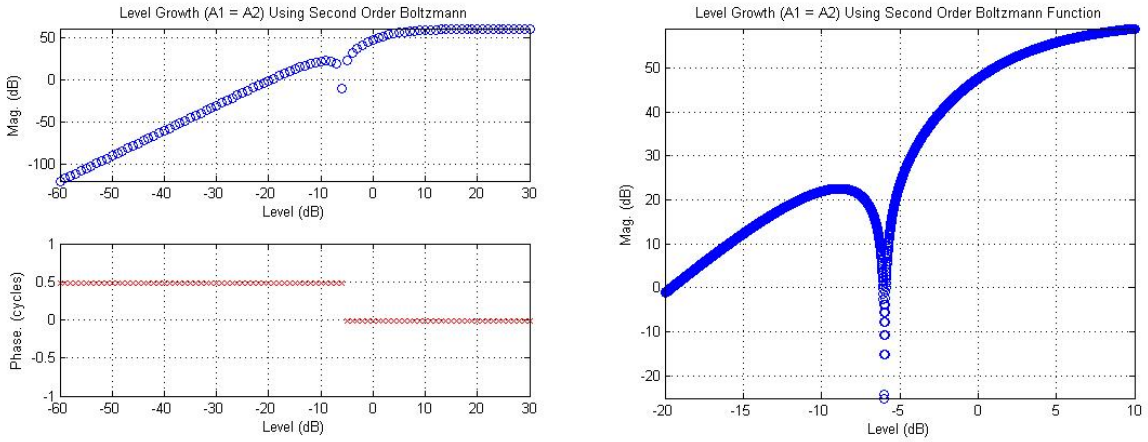

Figure 4: The level growth for the distortion product with frequency $2f_1 - f2$ using the the second order Boltzmann function. The graph on the right shows a more detailed image of the notch.

7 Analytical Exploration of Growth Properties of Nonlinear Distortion

In order to analytically explore the problem, the method outlined in section 4 will be used to derive an equation for the magnitude of the distortion products. The transducer input-output function $y(x)$ will be expanded into a Taylor's series about the operating point like in Eq. (5). By substituting the x of Eq. (2) into Eq. (5), the output magnitude for a specific frequency can be found. This method requires an approach similar to the method used to find Eq. (4). The value of x for different powers is calculated, and the coefficients of the cosine functions with the chosen frequency are extracted from the result. From Eq. (4) for example, the term

$$y(x) = \frac{3}{4} A_1^2 A_2 \tag{8}$$

would be selected if the desired distortion frequency were $2\theta_1 - \theta_2$. Continuing this process for higher values of n for $2\theta_1 - \theta_2$ would yield

$$y_{2f_1-f_2}(x) = A_1^2 A_2 \left[\frac{3}{4}a_3 + \frac{5}{8}a_5(2A_1^2 + 3A_2^2) + \frac{105}{64}a_7(A_1^4 + 4A_1^2A_2^2 + 2A_2^4) + \cdots\right] \quad (9)$$

By setting A_1 equal to A_2, the equation can also be written as

$$y_{2f_1-f_2}(x) = \frac{3}{4}a_3A^3 + \frac{25}{8}a_5A^5 + \frac{735}{64}a_7A^7 + \cdots \quad (10)$$

The relative weight of each term is dependent on the peak amplitudes of the primary input signals. The output of this equation should be similar to the numeric estimate as they are different approaches to model the same non-monotonic growth. A MATLAB program was created to graph this equation using these three terms. The graph for these three terms is shown in Fig. 5.

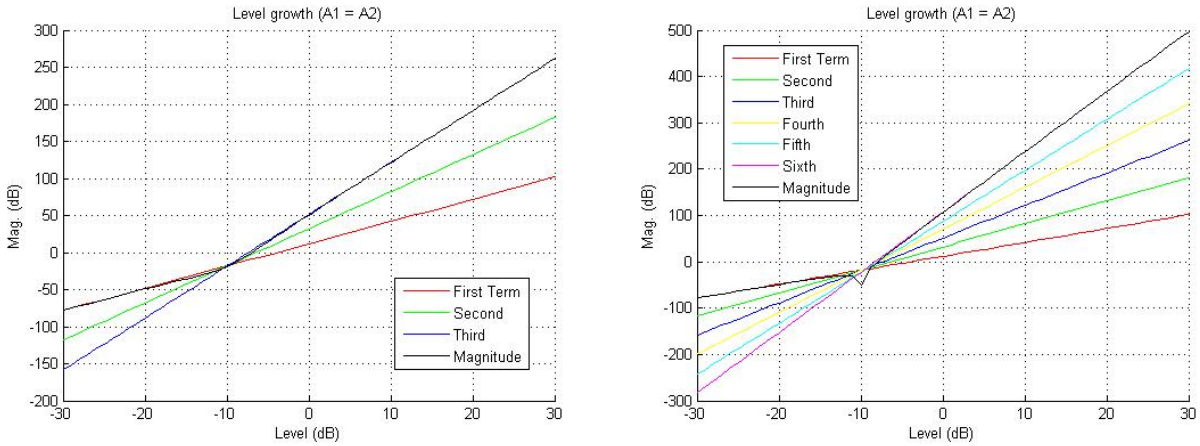

Figure 5: The magnitude of the distortion product with frequency $2f_1 - f_2$ for different levels of input. The graphs show the contribution of each term in the analytical equation. The magnitude is the sum of the individual terms in the function. These graphs do not share the characteristics of the non-monotonic growth found in actual DPOAE data.

7.1 Explanation of Error in Graph

The first graph in Fig. 5 does not agree with the data or the numerical model. The notch is not evident in the output and it does not saturate at higher levels. The function continues to grow linearly with a slope of 7. Since the units of the graph

are in decibels, this slope indicates that the model is growing to the seventh power. From Eq. (10), it is obvious that the third term eventually dominates the equation. The output does initially have the cubic growth. From Eq. (10), it is obvious that the first term dominates in this region. One potential cause for the inconsistencies between the graphs and the expected results is that not enough terms were used in the equation. Eq. (10) seems to behave like an alternating series due to alternating signs in a_n coefficients. The number of terms would then have a major impact on the outcome of the graph. Three more terms were added to the equation and the resulting graph is shown in Fig. 5. These new terms were calculated using an equation derived by Lin Bian, Mark E Chertoff, and Emily Miller [3] to more easily calculate the coefficients. This equation is

$$y_{2f_1-f_2}(x) = \left[\sum_{n=3}^{\infty}\left[\frac{y^{(n)}(x_{op})}{2^{n-1}n!}\sum_{k=1}^{n}\left[A_1^{n-k-2}A_2^{k-1}\binom{n}{k}\binom{n-k}{i}\binom{k}{j}\right]\right]\right] \tag{11}$$

The n term represents the odd order power of the level and the k term represents the coefficients of that level and power. The $\binom{n}{k}$ represents the binomial coefficient of n and k. The second graph using more terms was a closer fit to the numerical estimate and the actual data. This output has an obvious notch. However, there is still no evidence of saturation. The function becomes dominated by the highest power once again after the notch. This indicates that many more terms may be needed in order to get a more accurate analytical estimate. Or, a new approach may need to be taken in regards to the initial set up of the equation.

8 Discussion

8.1 Relation to Hearing/OAEs

The exploration demonstrates that for a simplified system, a single source model is sufficient to produce the characteristics found in actual DPOAE data. The simplified system consisted of a single hair cell and the input signals to that hair cell. The numerical model was able to replicate the characteristics of non-monotonic growth for DPOAEs well. Our results indicate that nonlinear hair cell transduction has an important effect on DPOAE generation.

8.2 Future Plans

Future plans for further research include resolving the disparity between the numerical and analytical estimates. The analytical model should achieve the same result as the numerical one. I hypothesize that the error in the analytical exploration is that too few terms were used to calculate the output.

Further research would also include analyzing real OAE data. One aspect of the data that requires further investigation is the phase cycle shifts that occur at notches. Actual data has phase shifts at the notches, but they are not always half a cycle [4]. This irregularity could be analyzed using additional models in an attempt to improve the understanding of how this change is possible.

A third path for possible research is analyzing OAEs from the ear as a whole instead of just the simplified system. OAEs are affected to a degree by other properties and characteristics of the ear. One such characteristic is the many hair cells present in the inner ear. Understanding how these single elements of hair cells work together would be interesting to investigate.

8.3 Summary of What I Have Learned

Over the course of this research, I have learned to read and analyze research journals. I've learned that it is important to critically examine ideas and look for flaws in the logic behind them. My understanding of complex numbers and Euler's equation has improved dramatically and helped me in several areas of math. My MATLAB and LaTeX programming skills have improved as well. They are useful tools for exploring mathematical concepts, performing calculations, and forming mathematical models. I've learned more about the auditory periphery and non-monotonic growth functions over the course of the research. I've improved my mathematical understanding of these ideas through analytically modeling them in their simplest form. In this research, we focused on a single distortion product which is a part of the general otoacoustic emissions generation process. By taking different approaches to investigating the distortion product, we developed a method to estimate the output of a variety of distortion products and began to gain a sense of the role that an OHC may play in this process. Each approach offers new tools and insights that will be useful in future analysis of distortion products and other OAEs.

Appendix - Technical Issues

Aliasing

In Fig. 3, the response spectrum incorrectly shows some of the frequencies. This is due to aliasing done by the program. Aliasing refers to the distortion of a signal that is sampled and reconstructed as an alias of the original signal. When the program reached the edge of its range, the data wrapped back around. Some of the magnitudes present in Fig. 3 should be at higher frequencies.

Analysis of the Error in Numerical Derivatives

A derivative is a measure of how the value of a function changes as its inputs are changed. The derivative of a function $f(x)$ is defined as

$$f'(x) = \lim_{h \to 0} \frac{f(x+h) - f(x)}{h} \tag{12}$$

Despite having a definite formula to calculate the derivative, determining the derivative numerically has inherent difficulties. One difficulty a computer experiences when calculating a derivative is how the numbers are represented in binary. In order for a computer to make the calculations necessary for a derivative, it often must add an error characteristic of its floating point format. While these changes are small, they have a significant impact on the derivative equation where the value of h is supposed to be approximately 0. This is a rounding error. The other error that arises when calculating the derivative is what value the calculator should set for h. The computer is unable to use h is equal to 0 because the function would then be undefined. The smaller the h value, the more susceptible it will be to the machine's characteristic error for performing calculations with numbers. If h is too large, a truncation error will occur. This can be demonstrated by Taylor's series expansion. The Taylor's series expansions for $f(x+h)$ around x is

$$f(x+h) = f(x) + hf'(x) + \frac{1}{2}h^2 f''(x) + \frac{1}{6}h^3 f'''(x) + \cdots \tag{13}$$

Substituting Eq. (13) into Eq. (12) gives

$$\frac{f(x+h) - f(x)}{h} = f'(x) + \frac{1}{2}hf''(x) + \frac{1}{6}h^2 f'''(x) + \cdots \tag{14}$$

When the value of h is close to zero, the terms right of $f'(x)$ become 0. When h is not sufficiently small enough, these terms affect the outcome of the derivative.

Numerical Derivatives in Programs

The error inherent in numerically calculating derivatives is especially detrimental to attempting to graph an equation that models the level-magnitude relationship of otoacoustic emissions. Eq. (10) calls for the calculation of many higher order derivatives. The error in derivative calculations is even greater for these higher order derivates necessary to create the graph. The error of each derivative is carried over and increased as additional derivatives are taken. Below are some graphs demonstrating the error in the derivatives of a hyperbolic tangent function, which is similar to the input-output function in the model. The formula for the function is $f(x) = a\tanh(b\mathrm{x}-c)+d$.

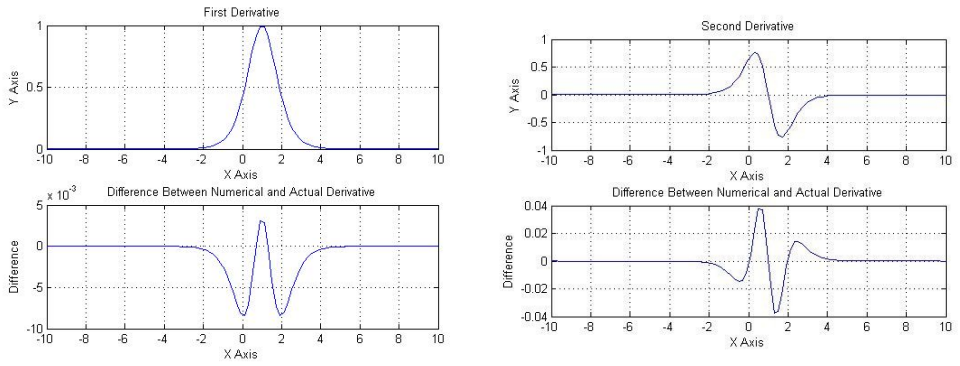

Figure 6: The error in the first and second derivative for a hyperbolic tangent function.

As these figures show, the error in the derivative becomes greater after each successive derivative. Calculating the general formula for each derivative would improve the accuracy of the program. Since accurate derivatives are crucial to analytically estimating distortion product magnitudes, calculating the actual derivative using another method is a better approach than using MATLAB's gradient program.

References

[1] Dallos, Peter. (**1992**) *The Active Cochlea.* The Journal of Neuroscience **112** (12), 4575-4585

[2] Lukashkin, Andrei N. and Ian J. Russell. (**1998**) *A descriptive model of the receptor potential nonlinearities generated by the hair cell mechanoelectrical transducer.* J. Acoust. Soc. Am. **103** (2), 973-980

[3] Lin Bian, Mark E. Chertoff, and Emily Miller. (**2002**) *Deriving a cochlear transducer function from low-frequency modulation of distortion product otoacoustic emissions.* J. Acoust. Soc. Am. **112** (1), 198-210

[4] Manfred Kossl, Frank Coro, Ernst-August Seyfarth, and Wolfgang A. Nassig. (**2007**) *Otoacoustic emissions from insect ears having just one auditory neuron.* J. Comp. Physiol. A.